

# Antimicrobial Activity of Peptidomimetics against Multidrug-Resistant *Escherichia coli*: A Comparative Study of Different Backbones

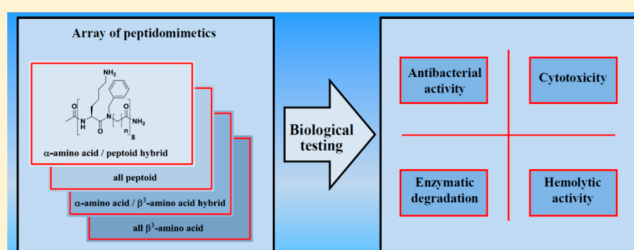
Rasmus D. Jahnsen,<sup>†</sup> Niels Frimodt-Møller,<sup>‡</sup> and Henrik Franzky<sup>\*†</sup>

<sup>†</sup>Department of Drug Design and Pharmacology, Faculty of Health and Medical Sciences, University of Copenhagen, Universitetsparken 2, DK-2100 Copenhagen, Denmark

<sup>‡</sup>Department of Microbiology, Hvidovre Hospital, Kettegaard Allé 30, DK-2650 Hvidovre, Denmark

**S** Supporting Information

**ABSTRACT:** Novel remedies in the battle against multidrug-resistant bacterial strains are urgently needed, and one obvious approach involves antimicrobial peptides and mimics thereof. The impact of  $\alpha$ - and  $\beta$ -peptoid as well as  $\beta^3$ -amino acid modifications on the activity profile against  $\beta$ -lactamase-producing *Escherichia coli* was assessed by testing an array comprising different types of cationic peptidomimetics obtained by a general monomer-based solid-phase synthesis protocol. Most of the peptidomimetics possessed high to moderate activity toward multidrug-resistant *E. coli* as opposed to the corresponding inactive peptides. Nevertheless, differences in hemolytic activities indicate that a careful choice of backbone design constitutes a significant parameter in the search for effective cationic antimicrobial peptidomimetics targeting specific bacteria.



## INTRODUCTION

Increased occurrence of multidrug-resistant (MDR) pathogenic bacterial strains is recognized as a serious health hazard.<sup>1</sup> Excessive use of antibiotics, both for treatment of humans and in livestock production,<sup>2</sup> together with a declining effort from pharmaceutical companies in pursuing development of new anti-infective agents,<sup>3</sup> have led to the emergence of untreatable infections. In particular, the drug development pipelines lack novel types of antibiotics against Gram-negative pathogens belonging to the *Enterobacteriaceae*. Notably, *Escherichia coli* have gained increased clinical importance due to the worldwide occurrence of MDR strains. Recent examples comprise extended-spectrum  $\beta$ -lactamase (ESBL)-producing *E. coli*<sup>4,5</sup> and New Delhi metallo- $\beta$ -lactamase-1 (NDM-1)-producing *E. coli*.<sup>6</sup> Consequently, medical organizations have stressed the urgent need for novel treatments of *E. coli* infections.<sup>7,8</sup> One approach involves searching for novel antibacterial agents with mechanisms of action different from those of traditional antibiotics. Natural antimicrobial peptides (AMPs) have for long been considered a potential source of such lead compounds as they constitute an essential part of the innate host defense immune system.<sup>9,10</sup> Although several sequence-modified AMPs have entered clinical trials,<sup>10</sup> the general challenges encountered in development of peptide drugs (e.g., low stability and limited bioavailability) also apply to AMPs.<sup>11</sup> To improve stability, a variety of backbone modifications have been implemented in the design of peptidomimetics. These include replacement of natural L-amino acids with: (i)  $\beta$ -amino

acids,<sup>12</sup> (ii) N-alkylated glycine residues (i.e.,  $\alpha$ -peptoids),<sup>13</sup> and (iii) N-alkylated  $\beta$ -alanine residues (i.e.,  $\beta$ -peptoids)<sup>14</sup> (Figure 1).

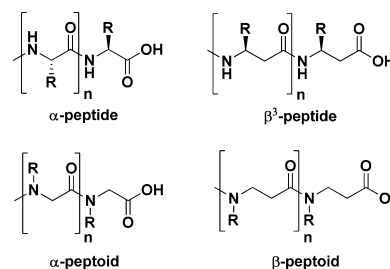


**Figure 1.** The backbone structure of a natural  $\alpha$ -peptide and common peptidomimetics.

Furthermore, there are indications that such modifications are associated with enhanced antimicrobial activity and/or decreased hemolytic activity.<sup>15–18</sup> Hence, we hypothesize that optimal backbone design indeed constitutes a valuable approach to improve the overall activity profiles (i.e., toxicity versus antimicrobial activity) of antimicrobial peptidomimetics. To corroborate this assumption, we here directly compare several backbone designs as such investigations appear to be lacking in the literature. Previously, we have reported on

Received: June 11, 2012

Published: July 18, 2012

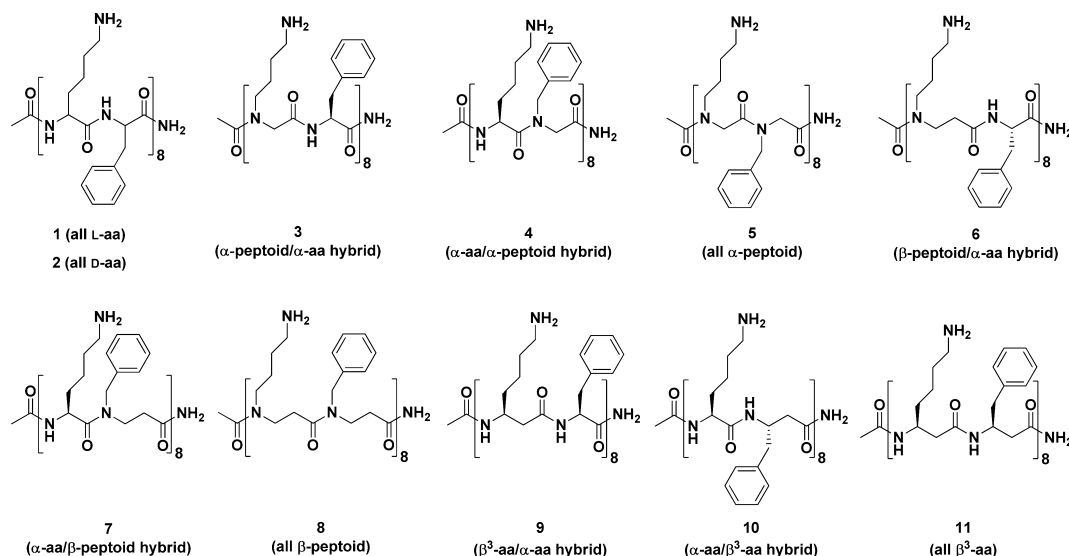


Figure 2. Peptides and peptidomimetics examined in the present work. aa: amino acid.

alternating hybrid sequences (composed of cationic  $\alpha$ -amino acids and hydrophobic  $\beta$ -peptoid residues) that exhibited antibacterial potency against *E. coli*.<sup>18,19</sup> In the present study, a similar alternating design was employed, but Lys was chosen over Arg as the cationic amino acid component of the peptidomimetics, as it usually is associated with a higher selectivity in the killing of bacteria over human cells.<sup>20</sup> Moreover, we included the all-L and all-D 16-mer peptides Ac-(Lys-Phe)<sub>8</sub>-NH<sub>2</sub> (i.e., 1 and 2) as reference compounds. Systematic incorporation of  $\alpha$ - and  $\beta$ -peptoid as well as  $\beta^3$ -amino acid residues gives rise to nine different peptidomimetics with modified backbones (3–11 in Figure 2). This array comprises three homotypic compounds (5, 8, and 11) as well as six hybrids containing L- $\alpha$ -amino acids and unnatural residues in a 1:1 ratio. Previous synthetic methodology involved tedious preparation of dimeric building blocks in solution prior to assembly on solid phase,<sup>19,21</sup> however, a more versatile monomer-based method using a common efficient coupling procedure is here established.

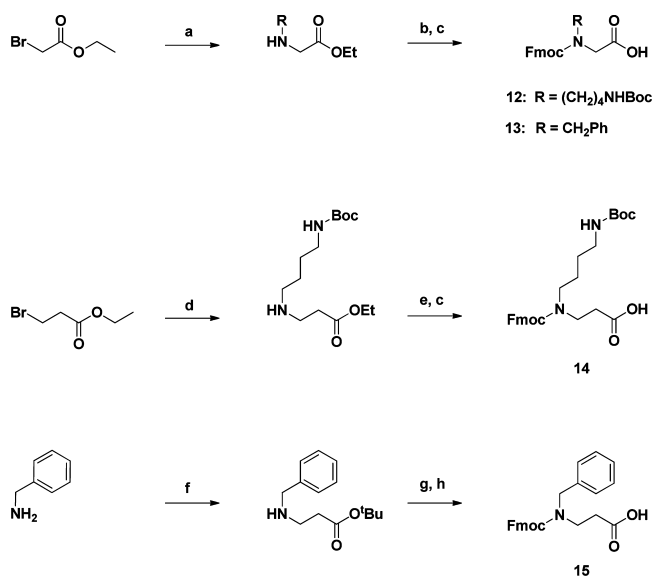
## RESULTS

### Versatile Solid-Phase Synthesis of Peptidomimetics.

Preliminary experiments showed that on-resin amide bond formation involving congested  $\alpha$ -chiral  $\beta$ -peptoid secondary amines and  $\alpha$ -amino acid building blocks is strongly hampered due to steric hindrance. Moreover, our previous work indicated that the degree of chirality of such peptidomimetics only had a minor influence on their antibacterial potency.<sup>18</sup> Hence, to fulfill our intention of using a common monomer-based microwave (MW)-assisted solid-phase peptide synthesis (SPPS) protocol for all peptidomimetics, we focused on incorporating less congested achiral peptoid residues. Consistent with these considerations, peptoid building blocks 12–15 with Lys- or Phe-like side chains were prepared as depicted in Scheme 1, while the corresponding  $\beta^3$ -peptide building blocks were obtained from a commercial supplier.

The required  $\alpha$ -peptoid building blocks for SPPS were prepared as previously described.<sup>22</sup> In brief, the appropriate primary amine was alkylated by using ethyl 2-bromoacetate, and subsequent hydrolysis and Fmoc protection yielded the desired monomer (12 or 13). Similarly, the  $\beta$ -peptoid Lys-like

### Scheme 1<sup>a</sup>



<sup>a</sup>Reagents and conditions for preparation of peptoid building blocks: (a) 1 equiv R-NH<sub>2</sub>, 3 equiv Et<sub>3</sub>N, rt, 24 h, s THF; (b) 1 equiv NaOH, rt, 30 min, s dioxane–MeOH 2.5:1; (c) 1 equiv Fmoc-OSu, rt, 30 min, s H<sub>2</sub>O–MeCN 1:2; (d) 1 equiv BocNH(CH<sub>2</sub>)<sub>4</sub>NH<sub>2</sub>, 3 equiv Et<sub>3</sub>N, initially 0 °C, then 5 °C, 72 h, s DCM; (e) 1 equiv NaOH, rt, 30 min, s dioxane–MeOH 2.5:1; (f) 2.0 equiv *tert*-butyl acrylate, 150 °C (MW), 2 h, s DMSO; (g) TFA–DCM 1:2, rt, 2 h; (h) 1.2 equiv Fmoc-Cl, initially 0 °C, then rt, 16 h, s dioxane–10% aq Na<sub>2</sub>CO<sub>3</sub> 1:1.

monomer 14 was prepared by alkylation of the appropriate amine with ethyl 3-bromopropanoate,<sup>23</sup> followed by saponification and Fmoc protection. The  $\beta$ -peptoid Phe-like monomer 15 was obtained via an aza-Michael addition approach as previously described.<sup>21</sup> Identity of the building blocks was validated by <sup>1</sup>H and <sup>13</sup>C NMR spectroscopy as well as by LC-HRMS, while purity (>95%) was determined by analytical HPLC.

MW-assisted assembly of oligomers on solid phase was performed via a standard Fmoc protocol by using a Rink amide resin. Screening of several coupling reagents (i.e., TFFH, HBTU, PyBOP, and DIC) and additives (HOAt and HOBT)

Table 1. MIC ( $\mu\text{M}$ ) of the Compounds<sup>a</sup>

compd	<i>E. coli</i>				<i>K. pneumoniae</i>		
	ATCC 25922	ESBL <sup>b</sup>	AmpC <sup>c</sup>	NDM-1	KPC-2	NDM-1	MRSA
1	>256	>256	>256	128	>256	>256	16
2	128	256	256	128	256	256	16
3	16	16	32	32	256	256	>256
4	4	8	8	2	128	128	256
5	32	64	32	32	256	256	256
6	8	16	16	2	64	256	256
7	8	4	8	4	128	256	>256
8	16	8	16	4	256	256	256
9	8	8	16	4	128	256	256
10	64	32	32	64	128	128	32
11	16	32	32	32	32	32	16
gentamicin	1.7	>111	6.9	>111	>111	111	56
cefotaxim	<0.1	>134	2.1	>134	>134	>134	34
ciprofloxacin	<0.1	>152	152	>152	152	152	19

<sup>a</sup>ESBL, extended-spectrum  $\beta$ -lactamase; NDM-1, New Delhi metallo- $\beta$ -lactamase-1; KPC-2, *Klebsiella pneumoniae* carbapenemase-2; MRSA, methicillin-resistant *Staphylococcus aureus*; MICs for compounds 1–11 were determined in the range of 0.25–256  $\mu\text{M}$ . <sup>b</sup>CTX-M-15. <sup>c</sup>CMY-2. MICs for control compounds were determined in the range of 0.062–64  $\mu\text{g}/\text{mL}$  (shown as the  $\mu\text{M}$  concentration for ease of comparison).

revealed that only the DIC/HOAt activator system<sup>24</sup> afforded satisfactory purities of all types of 16-mer peptidomimetics. The resin-bound oligomers were then subjected to simultaneous deprotection and cleavage from the resin with TFA/ $\text{CH}_2\text{Cl}_2$ . Product isolation was performed by preparative HPLC, while purity and identity were validated by analytical HPLC (>95%) and LC-HRMS, respectively.

**Antibacterial Activity against MDR Strains of the Enterobacteriaceae, Cytotoxicity against Mammalian Cells, and Stability of Peptidomimetics.** The microbiological characterization of the peptidomimetic oligomers, reference peptides, and control substances (gentamicin, cefotaxim, and ciprofloxacin) involved determination of minimal inhibitory concentrations (MICs) against a standard laboratory *E. coli* strain (ATCC 25922) as well as against three MDR *E. coli* isolates comprising an ESBL-producing strain, an AmpC-producing strain, and an NDM-1-producing strain (Table 1). In addition, two MDR isolates of *Klebsiella pneumoniae* comprising a *K. pneumoniae* carbapenemase (KPC)-producing strain and an NDM-1-producing strain were included to estimate the selectivity of peptidomimetics among pathogenic Gram-negative bacteria (Table 1). Also, a methicillin-resistant *Staphylococcus aureus* (MRSA) isolate was in the test panel in order to confirm earlier observations<sup>18,19</sup> that lysine-containing peptidomimetics with a cationic/hydrophobic alternating design possess poor activity against Gram-positive pathogens (Table 1). The results showed that several of the tested peptidomimetics (4 and 6–9) were potent inhibitors of *E. coli* growth (MICs: 2–16  $\mu\text{M}$ ), particularly against the NDM-1-producing strain (MICs: 2–4  $\mu\text{M}$ ). In contrast, the  $\alpha$ -peptide (1) exhibited no activity (MIC > 256  $\mu\text{M}$ ), while the proteolytically stable all-D analogue (2) showed very low activity against all Gram-negative strains. In addition, some peptidomimetics (3, 5, 10, and 11) exhibited intermediate potencies with MICs against *E. coli* strains within the range 16–64  $\mu\text{M}$ . Also, the all- $\alpha$ -peptidic sequence generally exhibited somewhat lower activity than the corresponding peptide–peptoid hybrids (i.e., 5 vs 3/4), whereas this trend was less pronounced for the  $\beta$ -peptoid-containing peptidomimetics. Among the peptidic hybrids, the highest antibacterial activity was observed when the unnatural

moieties constituted the hydrophobic residues (i.e., 3 vs 4 and 6 vs 7). In general, the peptidomimetics exhibited significantly lower activity against *K. pneumoniae* (with the all- $\beta$ -peptide 11 as the only moderately active compound). The control substances exhibited activity profiles as expected (i.e., absence of growth inhibition of the  $\beta$ -lactamase-producing *E. coli* strains). Interestingly, peptoid-containing peptidomimetics were all inactive against MRSA, while the  $\alpha$ - and  $\beta$ -peptides exhibited moderate activity (MICs: 16  $\mu\text{M}$ ). This confirmed overall selectivity against *E. coli* for alternating peptoid-containing peptidomimetics displaying amino-functionalized side chains.

To enable an assessment of the selectivity of the tested compounds toward bacteria over mammalian cells, their hemolytic activity was investigated (Table 2) as previously described.<sup>15</sup> Except for peptides 1 and 2, only peptidomimetics 9–11, containing  $\beta^3$ -amino acids, showed significant hemolytic activity, suggesting that these backbone designs to a somewhat

Table 2. Cytotoxicity, Selectivity, and Stability

compd	HA <sub>10</sub> [ $\mu\text{M}$ ] <sup>a</sup>	TI <sup>b</sup>	IC <sub>50</sub> [ $\mu\text{M}$ ] <sup>c</sup>	protease stability <sup>d</sup>
1	<1	<0.004	19.6 $\pm$ 1.2	–
2	<1	<0.008	18.1 $\pm$ 1.2	+
3	>128	>5	266.7 $\pm$ 14.5	(+) <sup>e</sup>
4	>128	>21	100.9 $\pm$ 4.3	+
5	>128	>4	194.3 $\pm$ 21.8	+
6	>128	>11	62.6 $\pm$ 1.2	+
7	>128	>21	25.9 $\pm$ 1.0	+
8	>128	>10	168.8 $\pm$ 8.5	+
9	64	8	132.8 $\pm$ 9.7	+
10	64	1	31.1 $\pm$ 3.9	+
11	128	4	31.0 $\pm$ 10.1	+

<sup>a</sup>The hemolytic activity (HA) is given as the concentration observed from a 2-fold dilution series that resulted in lysis of at least 10% red blood cells. <sup>b</sup>The therapeutic index (TI) was calculated as the HA divided by the median of the MIC values. <sup>c</sup>The toxicity against HeLa cells is given as IC<sub>50</sub> value for inhibiting growth of HeLa cells. The highest concentration tested was 1024  $\mu\text{M}$ . <sup>d</sup>The susceptibility for enzymatic degradation was tested against Pronase. <sup>e</sup>The degradation product detected after 50 h was investigated by HRMS.

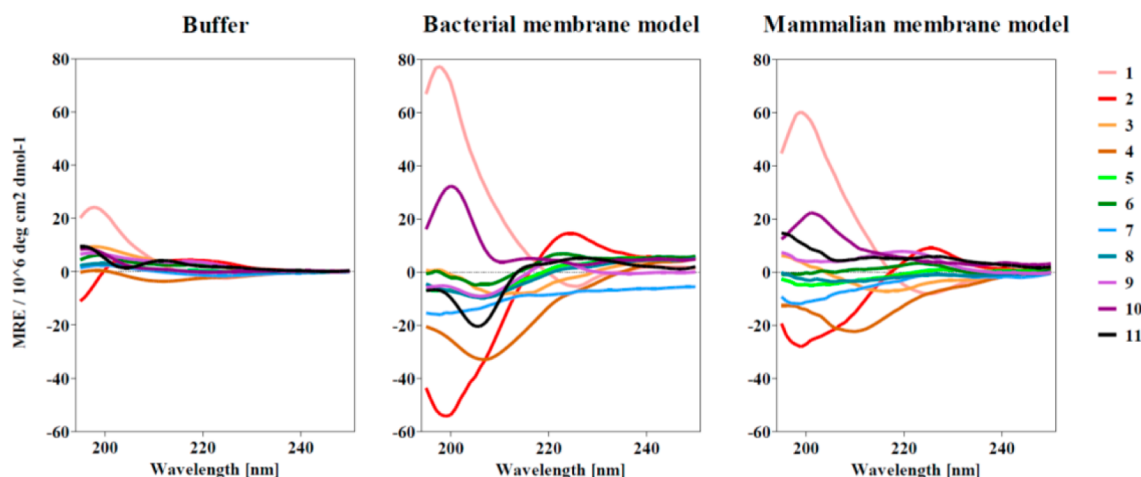


**Figure 3.** Circular dichroism data shown as mean residue ellipticity (MRE) signals for spectra obtained in buffer as well as in the presence of lipid vesicles modeling a bacterial membrane and a mammalian membrane, respectively.

higher degree confer hemolytic properties to peptidomimetics with alternating cationic/hydrophobic sequences.

All modifications induced reduction in the ability to kill HeLa cells. In particular, hybrids with modifications in the cationic residue had an increased  $IC_{50}$  value as compared to the hydrophobic residue-modified counterpart (compounds **3** vs **4**, **6** vs **7**, and **9** vs **10**). Also, the  $\alpha$ -peptoid-modified compounds in general exhibited lower toxicity than the  $\beta$ -peptoid and  $\beta^3$ -amino acid-containing compounds.

The proteolytic stability of the peptidomimetics and reference peptides (Table 2) was investigated by using a Pronase degradation assay monitored by reverse-phase HPLC.<sup>15</sup> In addition to the expected fast extensive degradation observed for  $\alpha$ -peptide **1**, hybrid **3** was converted into a single slightly more polar compound, which by LC-HRMS analysis was shown to arise by cleavage of the C-terminal Phe residue. All other compounds were found to be stable.

**Structural Features Observed in the Presence of Model Membranes.** The degree of secondary structure of the oligomers was assessed by circular dichroism (CD) spectroscopy. Large unilamellar phospholipid vesicles (LUVs) with varied contents of zwitterionic and negatively charged phospholipids were employed as model systems for biological membranes. A lipid mixture composed of zwitterionic 1-palmitoyl-2-oleoyl-*sn*-glycero-3-phosphocholine (POPC) and negatively charged 1-palmitoyl-2-oleoyl-*sn*-glycero-3-phosphoglycerol (POPG) in a ratio of 3:7 was used as a simple model for the bacterial membrane, while a mixture of POPC, POPG, and cholesterol in the ratio 5:3:2 served as a model of a mammalian cell membrane.<sup>25</sup> Circular dichroism spectra for all compounds were obtained in buffer (pH 7.4) as well as in the presence of the above lipid model systems (Figure 3). In the absence of lipid vesicles, the compounds exhibited low mean residue ellipticity (MRE) intensity in their CD spectra obtained in buffer. In contrast, as depicted in Figure 3, the presence of both model membranes induced various degrees of secondary structure. In the bacterial membrane model, peptides **1** and **2** exhibited relatively high numerical MRE around 200 nm ( $60000\text{--}80000 \times 10^{-6} \text{ deg cm}^2 \text{ dmol}^{-1}$ ), while the peptidomimetics only showed moderate if any intensity increase at all. A similar pattern was observed in the mammalian membrane model, with peptides **1** and **2** demonstrating relatively high MRE ( $30000\text{--}60000 \times 10^{-6} \text{ deg cm}^2 \text{ dmol}^{-1}$ )

as compared to the peptidomimetics. It is noticeable that peptides **1** and **2**, which are associated with low antibacterial activity, high hemolytic activity, and high cytotoxicity, exhibited the most intense signals in both membrane model systems, suggesting that a high degree of secondary structure is not favorable for this particular side chain sequence.

## DISCUSSION AND CONCLUSIONS

Even though different structural modifications previously have been utilized as important design tools,<sup>26</sup> optimization of antibacterial peptidomimetics has usually focused on improvement of the nature of the side chains in a particular design instead of on direct comparison of several different types of backbone modifications. Thus, we were intrigued to investigate this seemingly unexplored structure–activity aspect systematically in order to assess the scope of backbone variation in optimization of peptidomimetics.

Focusing on clinically important Gram-negative pathogens belonging to the *Enterobacteriaceae*, we selected three *E. coli* MDR strains that are considered severe health challenges.<sup>27,28</sup> These clinical isolates exhibit resistance against several common classes of antibiotics including fluoroquinolones, aminoglycosides, and cephalosporins. Nevertheless, growth inhibition of the MDR *E. coli* strains by the most potent oligomers was observed at concentrations comparable to the MIC of the clinically relevant control gentamicin against the susceptible strain. Also, the activity of the oligomers seems completely unaffected by the  $\beta$ -lactamase phenotypic features, as the activity of each compound does not vary significantly between the tested *E. coli* strains. The activity toward both the *K. pneumoniae* and the MRSA strains generally was very low for most of the tested peptidomimetics, indicating selectivity against *E. coli* in accordance with previous indications for alternating sequences of Lys and Phe-like residues.<sup>18</sup>

Obviously, the choice of primary sequence is of major concern when developing AMP mimetics, but the present results demonstrate that further advancement most conveniently should include backbone variation. Thus, comparison of peptidomimetics **3–11** with peptides **1** and **2** revealed that incorporation of any of the selected unnatural amino acid analogues resulted in significant enhancement of both potency and selectivity, whereas the all-D analogue **2** only was slightly more active than **1**. This clearly suggests that proteolytic

stability is only of minor importance as compared to an altered backbone design that may allow for a different mode of displaying the side chain functionalities. In addition, it was demonstrated that replacement of every second residue in the peptide sequence with unnatural moieties may confer improved properties to the analogues to the same extent as seen for an entirely peptidomimetic sequence (i.e., 4 vs 5, 6/7 vs 8, and 9 vs 11).

Folding may allow AMPs to adopt amphiphilic structures, and traditionally this propensity has been closely linked to their mode of action. Although, the mechanism of AMPs is not fully understood, there is consensus that it involves some degree of membrane disruption resulting in either access to intracellular targets, lysis, or partial efflux of essential cell contents.<sup>29</sup> The achiral backbone of peptoids lacks hydrogen bond donors, excluding stabilization via interchain hydrogen bonds similar to those promoting  $\alpha$ -helical peptide structures. Regardless, peptoid oligomers may in fact adopt well-defined secondary structures provided the sequence has a high abundance of residues with  $\alpha$ -chiral side chains.<sup>17,19,30,31</sup> However, a globally amphiphilic secondary structure appears not to be a prerequisite for antimicrobial peptidomimetics to exhibit favorable activity profiles because irregular but amphiphilic conformations may be induced by interactions with membranes.<sup>15,32</sup> This implication that a well-defined secondary structure might be of less importance than traditionally assumed was supported by our recent work indicating that exchange of  $\alpha$ -chiral peptoid residues with achiral counterparts in alternating  $\alpha$ -amino acid/ $\beta$ -peptoid sequences does not compromise their potency against *E. coli*.<sup>18</sup> Also, the present results further corroborate the hypothesis that antibacterial activity of cationic/hydrophobic alternating peptidomimetics seems to be independent of a high degree of secondary structure. The exact relationship between the modifications and the increased activity on a mechanistic level remains to be resolved. Yet, the MIC values found in the present study suggest that flexibility is essential for antimicrobial activity. Almost all modes of action proposed for AMP-induced bacterial killing involves an initial conformational change upon interaction with bacterial membranes, and therefore molecular flexibility is believed to play a key role. Although oligomers containing  $\beta^3$ -amino acids may adopt well-defined secondary structures, their possible conformational space relative to the corresponding  $\alpha$ -peptide is increased due to additional torsional freedom of the backbone, thus decreasing the folding propensity of  $\beta^3$ -peptides.<sup>33</sup> This ultimately suggests that these oligomers are less rigid as compared to  $\alpha$ -peptides. Similarly, peptoid oligomers possess a greater diversity of conformational states than  $\alpha$ -peptides due to their achiral nature and location of the side chains on the amide nitrogen atoms as well as the lack of hydrogen bond donors in the backbone.<sup>34</sup> Thus, it is noticeable that whenever flexibility was increased by incorporation of peptoid ( $\alpha$ - or  $\beta$ -) or  $\beta^3$ -amino acid residues, the hemolytic activities of the resulting analogues were decreased as compared to that of the reference peptides (i.e., 1/2 vs 3–11). These findings reflect that the mechanisms for killing of bacterial and mammalian cells differ and that the latter clearly is favored by a more rigid overall conformation.

As a measure for the selectivity toward bacteria over human cells, a therapeutic index (TI) was calculated (Table 1) as the ratio between antibacterial and hemolytic activity;<sup>35–37</sup> however, because most of the investigated peptidomimetics

did not exhibit significant hemolytic activity within the test range, the TI appears only useful as a ranking tool. Thus, hybrids 4 and 7 exhibited the most favorable TIs, indicating that alternating sequences displaying Lys as chiral cationic components and  $\alpha$ - and  $\beta$ -peptoid hydrophobic residues possess the best overall activity profile. Yet, if cytotoxicity against HeLa cells is considered a measure for toxicity against healthy mammalian cells, it is apparent that hybrid 4 would be the more promising candidate for further optimization (IC<sub>50</sub> [ $\mu$ M]: 100.9  $\pm$  4.3 for 4 vs 25.9  $\pm$  1.0 for 7). Still, toxicity against HeLa cells compared to hemolytic activity has recently been interpreted as a measure of selective antitumor activity.<sup>38</sup> Interestingly, incorporation of  $\beta$ -peptoids (i.e., hybrids 6 and 7) or hydrophobic  $\beta^3$ -amino acids (i.e., compounds 10 and 11) enhances this selectivity. Especially, hybrid 7 possesses a putative anticancer activity maintaining a significantly reduced hemolytic activity. These observations indicate that peptoid modifications also may constitute a relevant tool in search of novel peptide-based anticancer leads. Comparison of peptides 1 and 2 suggests that susceptibility to proteolytic degradation only has a minor impact on antibacterial potency. Moreover, the similarly high hemolysis and cytotoxicity against HeLa cells induced by peptides 1 and 2 indicate that interaction with human cells occurs without participation of specific receptors or other chiral discrimination. Notably, the C-terminal Phe residue in hybrid 3 was cleaved off upon degradation with Pronase, whereas the other two oligomers 6 and 9 containing the same C-terminal residue retained high stability.

Frequently, overall hydrophobicity has been correlated directly to antibacterial potency,<sup>35</sup> and consequently this possible relationship was examined: Figure 4 depicts the potency of the compounds as 1/MIC plotted against the retention time on an HPLC C<sub>18</sub> column as a simple measure for their hydrophobicity, however, no obvious correlation was inferred. In addition, a possible relationship between cytotoxicity against HeLa cells and hydrophobicity was investigated (Figure 4), but again no obvious correlation was inferred. This clearly indicates that overall hydrophobic properties only account for a minor contribution to the level of activity, while other factors (e.g., flexibility) are primary activity determinants.

Another perspective of the present work concerns the availability and cost of building blocks versus activity profiles of the final peptidomimetics. While a variety of both types of peptoids are readily obtained via relatively inexpensive, simple synthetic routes, the diversity of expensive commercial  $\beta^3$ -amino acids is limited, and their synthesis is quite tedious.<sup>35</sup> By contrast, a vast number of diverse hydrophobic  $\alpha$ -amino acid building blocks are available at a reasonable cost. This study has clearly demonstrated that cationic/hydrophobic alternating sequences with a 1:1 ratio of unnatural and natural residues may exhibit equally favorable properties as the corresponding entirely peptidomimetic sequences. Thus, future antimicrobial peptidomimetic designs most conveniently may comprise cationic peptoid residues, while side chain diversity may be introduced via hydrophobic  $\alpha$ -amino acids.

Evidently, several properties must be carefully balanced when deciding which type of design to advance further in an optimization process. The present work supports earlier findings that peptidomimetics in general appear superior to peptides as potential antibacterial agents, but their ranking and selectivity appear to depend on the specific bacterial target, and thus the conclusion of this comparative study mainly concerns

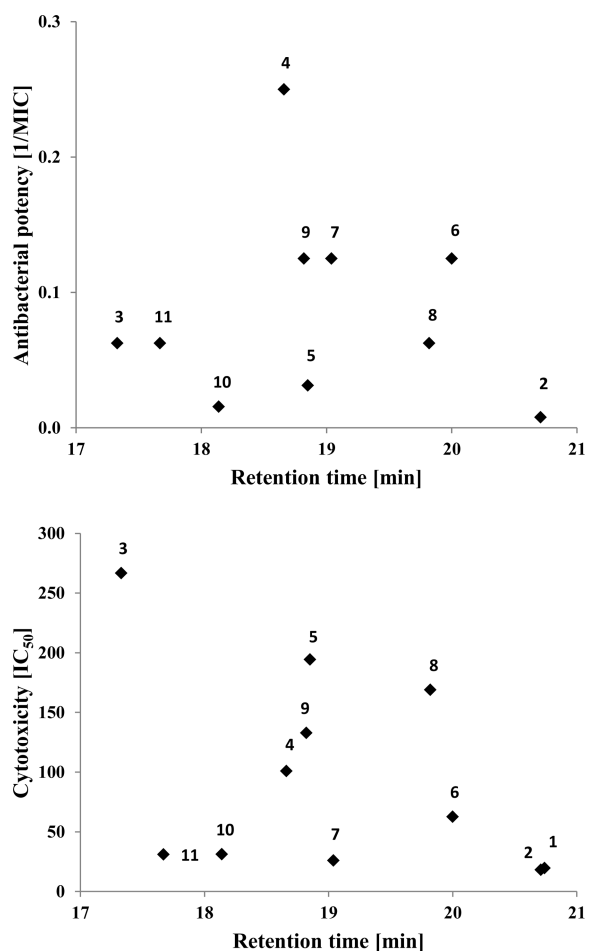


**Figure 4.** Antibacterial potency and cytotoxicity, respectively, plotted against hydrophobicity (as estimated by the retention time on a reversed phase HPLC column). The MIC against the ATCC 25922 strain was used in the calculation of 1/MIC.

*E. coli* for which the Lys/Phe-type designs proved valuable as all the tested clinically important MDR *E. coli* strains were highly susceptible to several of these peptidomimetics. As in many other studies, potency against Gram-negative bacteria was not associated with similarly high activities against Gram-positive bacteria, reflecting their different membrane structures.<sup>16–18,35</sup> However, it may be envisioned that similar comparative investigations of different types of peptidomimetic backbones may prove to be a powerful general strategy, e.g., in the search for stable alternatives to peptide leads that display a favorable combination of enhanced antibacterial activity and low toxicity.

## EXPERIMENTAL SECTION

Starting materials and solvents were purchased from commercial suppliers (Alfa Aesar, CHEMsolute, Iris Biotech GmbH, Sigma Aldrich, VWR, AppliChem, Fluka, ABCR GmbH, LabScan, and Merck) and used without further purification. <sup>1</sup>H and <sup>13</sup>C NMR spectra were recorded on Mercury Plus (300 MHz) and Varian Gemini 2000 (75 MHz) spectrometers, respectively. The residual solvent peak was used as internal reference (CDCl<sub>3</sub>: δ<sub>H</sub> = 77.16; δ<sub>C</sub> = 77.26), coupling constants (*J* values) are given in hertz (Hz). Multiplicities are reported as follows: singlet (s), doublet (d), triplet (t), quartet (q), pentet (pent), multiplet (m), and broad (br). Additional peaks due to the presence of a minor rotamer are designated \*. Water used during analytical and preparative HPLC was filtered through a 0.22 μm membrane filter. Analytical HPLC was used to determine purity and was carried out on a Phenomenex Luna C18

(2) (3 μm) column (150 mm × 4.6 mm) using binary mixtures of eluent A (water–MeCN–TFA 95:5:0.1) and eluent B (water–MeCN–TFA 5:95:0.1) for elution with a flow rate of 0.8 mL/min. Building blocks: linear gradient of 0–80% B during 5 min followed by a linear rise to 100% B during 25 min. Peptides and peptidomimetics: a linear gradient of 10–60% B during 30 min. UV-detection: building blocks at λ = 254 nm and peptides at λ = 220 nm. All compounds had a purity of at least 95%. Preparative HPLC was performed by using a Luna C18 (2) (5 μm) column (250 mm × 21.2 mm) on an Agilent 1100 LC system with a multiple-wavelength UV detector. Depending on the peptide, elution was performed with a linear gradient of 10–25% B, 10–30% B, 10–35% B, or 10–40% B during 20 min at a flow rate of 20 mL/min. Peptides were detected at λ = 215 and λ = 254 nm. LC-HRMS was performed with a Phenomenex Luna C18 (2) (3 μm) column (150 mm × 4.6 mm) using binary mixtures of eluent C (water–MeCN–formic acid 95:5:0.1) and eluent D (water–MeCN–formic acid 5:95:0.1). Elution was performed with a linear gradient of 10–60% D during 30 min at a flow rate of 0.5 mL/min. HRMS spectra were obtained by using a Bruker MicrOTOF-Q II Quadrupole MS detector. The analyses were performed as ESI-MS (*m/z*): [M + 5H]<sup>5+</sup> or [M + 6H]<sup>6+</sup> for peptidomimetics and [M + H]<sup>+</sup> for building blocks.

**Synthesis of *N*-(Boc-4-aminobutyl)-*N*-Fmoc Glycine (Compound 12).** The synthesis was carried out as previously described.<sup>22</sup> The yield from 10.0 g of mono-Boc-protected 1,4-butanediamine was 11.6 g (53%) of product 12; *t*<sub>R</sub> = 14.44 min (98.7% at 254 nm). HRMS: calcd for C<sub>26</sub>H<sub>32</sub>N<sub>2</sub>O<sub>6</sub> [M + H]<sup>+</sup> 469.2333, found 469.2318; Δ*M* = 3.2 ppm. <sup>1</sup>H NMR (300 MHz, CDCl<sub>3</sub>): δ = 1.10–1.60 (m, 4 H, CH<sub>2</sub>CH<sub>2</sub>), 1.45 (s, 9 H, C(CH<sub>3</sub>)<sub>3</sub>), 2.90–3.40 (m, 4 H, BocNCH<sub>2</sub> and FmocNCH<sub>2</sub>), 3.90, 3.95 (two br s, 2 H, NCH<sub>2</sub>C(O)), 4.10–4.25 (m, 1 H, CH-Fmoc), 4.40, 4.55 (two m, 2 H, CH<sub>2</sub>-Fmoc), 7.20–7.45 (m, 4 H, ArH-Fmoc), 7.50–7.60 (m, 2 H, ArH-Fmoc), 7.70–7.80 (m, 2 H, ArH). <sup>13</sup>C NMR (75 MHz, CDCl<sub>3</sub>): δ = 25.2\*, 25.5, 27.3, 28.6 (3C), 40.3, 41.6\*, 47.4, 48.2\*, 48.6, 49.1\*, 67.3, 67.8\*, 79.5, 120.0 (2C), 124.8 (2C), 125.0\*, 127.1 (2C), 127.7 (2C), 141.3 (2C), 141.4\* (2C), 143.9 (2C), 156.0, 156.6, 173.6.

**Synthesis of *N*-Benzyl-*N*-Fmoc Glycine (Compound 13).** The synthesis was carried out as previously described.<sup>22</sup> The yield from 5.4 g of benzylamine was 7.8 g (52%) of product 13; *t*<sub>R</sub> = 14.31 min (98.6% at 254 nm). HRMS: calcd for C<sub>26</sub>H<sub>32</sub>N<sub>2</sub>O<sub>6</sub> [M + H]<sup>+</sup> 388.1543, found 388.1549; Δ*M* = 1.6 ppm. <sup>1</sup>H NMR (300 MHz, CDCl<sub>3</sub>): δ = 3.78, 4.02 (two s, 2 H, NCH<sub>2</sub>C(O)), 4.20–4.35 (m, 1 H, CH-Fmoc), 4.50–4.65 (m, 4 H, CH<sub>2</sub>-Ph and CH<sub>2</sub>-Fmoc), 7.05–7.45 (m, 9 H, ArH-Fmoc and Ph), 7.50–7.60 (m, 2 H, ArH-Fmoc), 7.70–7.80 (m, 2 H, ArH-Fmoc). <sup>13</sup>C NMR (75 MHz, CDCl<sub>3</sub>): δ = 47.0\*, 47.3, 47.5, 47.9\*, 51.3, 51.5\*, 67.9\*, 68.2, 120.0 (2C), 124.8\* (2C), 124.9 (2C), 127.1 (2C), 127.6 (2C), 127.7\*, 127.8\*, 128.2 (2C), 128.8\*, 128.8 (2C), 136.3 (2C), 136.4\* (2C), 141.3 (2C), 143.7 (2C), 143.7\*, 156.3\*, 156.6, 175.0, 175.1\*.

**Synthesis of *N*-(Boc-4-aminobutyl)-*N*-Fmoc β-Alanine (Compound 14).** mono-Boc-protected 1,4-butanediamine (9.35 g) was dissolved in DCM (200 mL). Et<sub>3</sub>N (15.04 g; 3.0 equiv) was added to the solution. Ethyl 3-bromopropionate (8.97 g; 1.0 equiv) was added dropwise to the solution under stirring at 0 °C. The mixture was kept at 5 °C for 72 h, and then the mixture was concentrated in vacuo and partly redissolved in DCM (50 mL). The mixture was filtered, and the filtrate was loaded onto a VLC column (height, 8.5 cm; diameter, 9.5 cm; column material, 60H silica gel, column pretreated with heptane). Gradient elution was carried out with DCM followed by DCM–MeOH 50:1 and DCM–MeOH–NH<sub>3</sub> 200:10:1. The appropriate fractions were concentrated in vacuo to yield the intermediate ethyl ester (8.2 g, 85%) as a yellow oil, which was dissolved in dioxane (55 mL) and MeOH (20 mL). Then 4*N* NaOH (3.98 mL; 0.98 equiv) was added dropwise, and then the mixture was stirred for 30 min and concentrated in vacuo to yield 7.85 g solid, which was dissolved in water (60 mL), and then Fmoc-OSu (9.38 g; 1.0 equiv) in MeCN (120 mL) was added. The mixture was stirred 16 h and concentrated in vacuo to remove MeCN. The mixture was acidified with 20% citric acid (350 mL). The aqueous phase was extracted with EtOAc (3 × 200 mL). The combined organic phases were washed with water (3 × 300 mL) and brine (300 mL), dried over Na<sub>2</sub>SO<sub>4</sub>, and concentrated in

vacuo to yield approximately 12 g of solid, which was dissolved in DCM (60 mL) and loaded onto a VLC column (height, 9.0 cm; diameter, 9.5 cm; column material, 60H silica gel, column pretreated with heptane). Gradient elution was carried out with heptane followed by heptane–EtOAc 1:1 and heptane–EtOAc–AcOH 50:50:0.1. The appropriate fractions were concentrated in vacuo to yield product **14** (3.38 g; 24%);  $t_R = 14.49$  min (97.0% at 254 nm). HRMS: calcd for  $C_{26}H_{32}N_2O_6$   $[M + H]^+$  483.2490, found 483.2482;  $\Delta M = 1.7$  ppm.  $^1H$  NMR (300 MHz,  $CDCl_3$ ):  $\delta = 1.10$ – $1.50$  (m, 4 H,  $CH_2CH_2$ ), 1.45 (s, 9 H,  $C(CH_3)_3$ ), 2.24, 2.55 (two br s, 2 H,  $CH_2C(O)$ ), 2.85–3.15, 3.15–3.35, 3.35–3.50 (three m, 6 H, BocNCH<sub>2</sub>, FmocNCH<sub>2</sub> and NCH<sub>2</sub>CH<sub>2</sub>C(O)), 4.20 (br s, 1 H, CH-Fmoc), 4.40–4.60 (m, 2 H, CH<sub>2</sub>-Fmoc), 7.25–7.45 (m, 4 H, ArH-Fmoc), 7.50–7.60 (m, 2 H, ArH-Fmoc), 7.70–7.80 (m, 2 H, ArH-Fmoc).  $^{13}C$  NMR (75 MHz,  $CDCl_3$ ):  $\delta = 25.5^*$ , 25.9, 27.3, 27.6 (3C), 33.3, 40.3, 41.3<sup>\*</sup>, 43.0, 43.9<sup>\*</sup>, 47.5, 47.8<sup>\*</sup>, 66.7, 67.1<sup>\*</sup>, 79.4, 120.0 (2C), 124.7 (2C), 127.1 (2C), 127.7 (2C), 141.4 (2C), 144.0 (2C), 156.0 (2C), 176.0.

#### Synthesis of *N*-Benzyl-*N*-Fmoc $\beta$ -alanine (Compound 15).

The *N*-benzyl- $\beta$ -alanine *tert*-butyl ester was prepared as previously described.<sup>21</sup> The ester (10.60 g) was treated with TFA–DCM (1:2, 75 mL) for 2 h. The mixture was concentrated in vacuo to yield a solid (13.20 g) that was dissolved in dioxane (300 mL), 10% Na<sub>2</sub>CO<sub>3</sub> (250 mL), and water (200 mL). Upon cooling to 0 °C, Fmoc-Cl (13.97 g; 1.2 equiv) in dioxane (50 mL) was added slowly. The mixture was stirred at rt for 16 h and was then diluted with water (600 mL) and extracted with EtOAc (2  $\times$  500 mL) and Et<sub>2</sub>O (500 mL). The aqueous layer was acidified with 4N HCl (100 mL) and extracted with EtOAc (3  $\times$  1000 mL). The combined organic phases were dried over Na<sub>2</sub>SO<sub>4</sub> and concentrated in vacuo to yield 15.19 g of crude product, which was dissolved in DCM (45 mL) and loaded onto a VLC column (height, 7.0 cm; diameter, 9.5 cm; column material, 60H silica gel, column pretreated with heptane). Gradient elution was carried out with heptane followed by heptane–EtOAc–AcOH 50:10:0.6 to 25:10:0.35. The appropriate fractions were concentrated in vacuo to yield product **15** (12.70 g; 70%);  $t_R = 14.76$  min (98.1% at 254 nm). HRMS: calcd for  $C_{26}H_{33}N_2O_6$   $[M + H]^+$  402.1700, found 402.1711;  $\Delta M = 2.7$  ppm.  $^1H$  NMR (300 MHz,  $CDCl_3$ ):  $\delta = 2.18$  (t,  $J = 7$  Hz, 1 H, CH<sub>A</sub>H<sub>B</sub>C(O)), 2.62 (t,  $J = 7$  Hz, 1 H, CH<sub>A</sub>H<sub>B</sub>C(O)), 3.25 (t,  $J = 7$  Hz, 1 H, NCH<sub>A</sub>H<sub>B</sub>CH<sub>2</sub>C(O)), 3.57 (t,  $J = 7$  Hz, 1 H, NCH<sub>A</sub>H<sub>B</sub>CH<sub>2</sub>C(O)), 4.15–4.30 (m, 1H, CH-Fmoc), 4.35–4.50 (m, 2 H, CH<sub>2</sub>-Ph), 4.50–4.60, 4.60–4.70 (two m, 2 H, CH<sub>2</sub>-Fmoc), 6.95–7.10 (m, 1 H, ArH-Fmoc), 7.10–7.20 (m, 1 H, ArH-Fmoc), 7.20–7.40 (m, 7 H, ArH-Fmoc and Ph), 7.40–7.50 (m, 1 H, ArH-Fmoc), 7.50–7.65 (m, 1 H, ArH-Fmoc), 7.70–7.80 (m, 2 H, ArH-Fmoc).  $^{13}C$  NMR (75 MHz,  $CDCl_3$ ):  $\delta = 33.0$ , 42.2<sup>\*</sup>, 43.4, 47.4, 47.6<sup>\*</sup>, 51.3, 67.2<sup>\*</sup>, 67.6, 120.0 (2C), 124.7<sup>\*</sup> (2C), 124.9 (2C), 127.2, 127.5 (2C), 127.7 (2C), 128.7 (2C), 137.3, 141.4 (2C), 143.8 (2C), 156.3 (2C), 177.2<sup>\*</sup>, 177.3.

#### General Procedure for Synthesis of Peptidomimetics.

Peptidomimetics were prepared by automated MW-assisted SPPS on a CEM Liberty microwave peptide synthesizer. Rink amide resin (loading: 1 mmol/g) was used for all compounds. Fmoc deprotection conditions: Excess 20% piperidine in DMF, initially 75 °C (MW), 30 s, subsequently 75 °C (MW), 180 s. Coupling conditions: 5.0 equiv of building block, 5.0 equiv DIC, 5 equiv HOAt, s DMF, 75 °C (MW), 15 min. Capping was applied after every fourth coupling: Excess Ac<sub>2</sub>O–DIPEA–NMP 1:2:3, 65 °C (MW), 30 s, repeated once. Final Fmoc deprotection of the *N*-terminus was followed by acetylation as described for capping above. Then, the resin was transferred to a Teflon filter vessel using DMF and DCM. Upon draining, the resin was washed with DCM. Cleavage and simultaneous side chain deprotection: Excess TFA–water 95:5 (3 mL), rt, 1 h. The filtrate was collected and the resin was eluted with DCM (2 mL), MeOH (2 mL), TFA–water 95:5 (2 mL), and DCM (2 mL). The combined filtrates were concentrated in vacuo and then coevaporated with toluene and MeOH (each 3  $\times$  5 mL). The crude product was purified by using preparative HPLC and concentrated in vacuo. Finally, the product was dissolved in water (1 mL) and lyophilized.

**Peptide 1.** Elution was performed with a linear gradient of 10–40% B during 20 min. Yield: 35 mg (15%);  $t_R = 20.74$  min (98.7%, at 220

nm). HRMS: calcd for  $[M + 5H]^{5+}$  453.2769, found 453.2778;  $\Delta M = 2.0$  ppm.

**Peptide 2.** Elution was performed with a linear gradient of 10–35% B during 20 min. Yield: 83 mg (37%);  $t_R = 20.71$  min (97.7%, at 220 nm). HRMS: calcd for  $[M + 5H]^{5+}$  453.2784, found 453.2785;  $\Delta M = 0.2$  ppm.

**Hybrid 3.** Elution was performed with a linear gradient of 10–25% B during 20 min. Yield: 19 mg (8%);  $t_R = 17.33$  min (96.8%, at 220 nm). HRMS: calcd for  $[M + 5H]^{5+}$  453.2800, found 453.2811;  $\Delta M = 2.4$  ppm.

**Hybrid 4.** Elution was performed with a linear gradient of 10–30% B during 20 min. Yield: 24 mg (11%);  $t_R = 18.66$  min (100%, at 220 nm). HRMS: calcd for  $[M + 5H]^{5+}$  453.2771, found 453.2773;  $\Delta M = 0.4$  ppm.

**Peptidomimetic 5.** Elution was performed with a linear gradient of 10–35% B during 20 min. Yield: 81 mg (36%);  $t_R = 18.85$  min (100%, at 220 nm). HRMS: calcd for  $[M + 5H]^{5+}$  453.2772, found 453.2776;  $\Delta M = 0.9$  ppm.

**Hybrid 6.** Elution was performed with a linear gradient of 10–35% B during 20 min. Yield: 31 mg (13%);  $t_R = 20.00$  min (100%, at 220 nm). HRMS: calcd for  $[M + 6H]^{6+}$  396.5867, found 396.5870;  $\Delta M = 0.8$  ppm.

**Hybrid 7.** Elution was performed with a linear gradient of 10–35% B during 20 min. Yield: 12 mg (10%);  $t_R = 19.04$  min (99.0%, at 220 nm). HRMS: calcd for  $[M + 6H]^{6+}$  396.5873, found 396.5887;  $\Delta M = 3.5$  ppm.

**Peptidomimetic 8.** Elution was performed with a linear gradient of 10–30% B during 20 min. Yield: 27 mg (22%);  $t_R = 19.82$  min (100%, at 220 nm). HRMS: calcd for  $[M + 6H]^{6+}$  415.2743, found 415.2750;  $\Delta M = 1.7$  ppm.

**Hybrid 9.** Elution was performed with a linear gradient of 10–30% B during 20 min. Yield: 45 mg (19%);  $t_R = 18.82$  min (98.5%, at 220 nm). HRMS: calcd for  $[M + 6H]^{6+}$  396.5865, found 396.5874;  $\Delta M = 2.3$  ppm.

**Hybrid 10.** Elution was performed with a linear gradient of 10–30% B during 20 min. Yield: 92 mg (39%);  $t_R = 18.14$  min (98.4%, at 220 nm). HRMS: calcd for  $[M + 5H]^{5+}$  475.7009, found 475.7011;  $\Delta M = 0.4$  ppm.

**Peptidomimetic 11.** Elution was performed with a linear gradient of 10–30% B during 20 min. Yield: 59 mg (24%);  $t_R = 17.67$  min (98.0%, at 220 nm). HRMS: calcd for  $[M + 5H]^{5+}$  498.1266, found 498.1265;  $\Delta M = 0.2$  ppm.

**In Vitro Antimicrobial Activity Experiment.** Minimal inhibitory concentrations (MIC) were determined by the microdilution broth method as previously described.<sup>39</sup> In brief, fresh overnight colonies were suspended to a turbidity of 0.5 McFarland units and were then further diluted in Mueller–Hinton BLII broth (Becton Dickinson). These bacterial suspensions were added to wells containing 2-fold serial dilutions of oligomers. The polypropylene trays (Nunc) were incubated at 35 °C in ambient air for 16–20 h. The MIC was determined as the lowest concentration showing no visible growth compared to the control without oligomer. The test range was 0.25–256  $\mu$ M.

**Assay for in Vitro Hemolytic Activity.** The lysis of human red blood cells was measured as previously described.<sup>15</sup> In brief, freshly drawn human red blood cells (hRBCs) were washed with TBS buffer (pH 7.2, 10 mM Tris, 150 mM NaCl) and centrifuged at 3400 rpm for 10 min. Two-fold serial dilutions of the oligomers in Milli-Q water were added to each well in a sterile round-bottom 96-well plate for a total volume of 20  $\mu$ L in each well. A 1% v/v hRBC suspension (80  $\mu$ L in TBS buffer) was added to reach a total volume of 100  $\mu$ L in each well. The plate was incubated (37 °C) for 1 h, and then the cells were pelleted by centrifugation at 3400 rpm for 5 min. The supernatant (80  $\mu$ L) was diluted with Milli-Q water (80  $\mu$ L), and hemoglobin was detected measuring the OD at 405 nm. OD of cells incubated with melittin (400  $\mu$ g/mL) defined 100% hemolysis, and OD of cells incubated with TBS buffer defined 0% hemolysis. The test range was 1–128  $\mu$ M.

**Assay for in Vitro Toxicity against HeLa cells.** Toxicity against HeLa cell viability was estimated as previously described.<sup>18</sup> In brief,

HeLa cells were seeded in flat-bottomed 96-well plates at a concentration of 9000 cells per well and cultured for 24 h under standard conditions. At 80–100% confluency, the cells were washed with HBSS and incubated (37 °C, 50 rpm) for 1 h with oligomers in 2-fold serial dilutions in EMEM. Upon washing the cells with HBSS (2 × 200 μL), freshly prepared MTS/PMS (240/2.4 μg/mL) reagent in HBSS (100 μL) was added to each well, and then incubation was continued for 1.5 h. The dehydrogenase activity was determined as a result of the amount of formazan produced as measured by the absorbance at 492 nm. The absorbance of cells incubated with 0.2% SDS defined 0% production of formazan, and absorbance of cells incubated with EMEM defined 100% production of formazan. For compounds 1, 2, 6, and 7, the test range was 1–128 μM, and for compounds 3, 4, 5, 8, 9, 10, and 11, it was 8–1024 μM.

**Determination of Protease Susceptibility.** Stability of peptides and peptidomimetics toward Pronase was investigated as previously described.<sup>15</sup> In brief, the enzyme activity of 1.0 mg/mL Pronase was confirmed by using the standard substrate *N*<sup>α</sup>-benzoyl arginine. Enzyme concentration sufficient for complete conversion of the standard substrate after 15 min was used. Each assay contained 10 mM Tris buffer (1.2 mL, pH 7.5), 1.0 mg/mL Pronase solution (50 μL), and 2 mg/mL oligomer solution (250 μL). Degradation was monitored by analytical HPLC (10–60% B) at *t*<sub>6 h</sub>, *t*<sub>12 h</sub>, *t*<sub>18 h</sub>, and *t*<sub>30 h</sub>. The degradation product of hybrid 3 originated from the cleavage of the C-terminal Phe and was identified by using HRMS: calcd for [M + 5H]<sup>5+</sup> 424.0600, found 424.0599; ΔM = 0.2 ppm.

**Preparation of Liposomes.** The LUVs were prepared from POPC and POPG in a 3:7 molar ratio or POPC, POPG, and cholesterol in a 5:3:2 molar ratio as previously described.<sup>25,40</sup> The particle size distribution was determined by dynamic light scattering by using the photon correlation spectroscopy technique. The measurements were performed on samples diluted five times in Tris buffer at 25 °C by using a Malvern ZanoZS (Malvern Instruments, Worcestershire, UK) equipped with a 633 nm laser and 173° detection optics. Malvern DTS 6.20 software (Malvern Instruments, Worcestershire, UK) was used for data acquisition and analysis.<sup>41</sup> All liposome preparations had a narrow size distribution with a mean diameter of approximately 100 nm. Determination of the lipid concentration was performed by using the Phospholipid B enzymatic colorimetric method. For this purpose, a Wako Phospholipids B kit (Wako Chemicals GmbH, Neuss, Germany) was acquired. In brief, the phospholipids were hydrolyzed to free choline by phospholipase D. The liberated choline was oxidized to betaine by choline oxidase with simultaneous production of hydrogen peroxide. The latter reacted quantitatively with 4-aminoantipyrine and phenol to form a compound with an absorption maximum at 505 nm. From a standard curve, the phospholipid concentration was calculated.

**Circular Dichroism Measurements.** For CD measurements, solutions of 20 μM compound in Tris buffer (pH 7.5) were used. In the experiments involving the membrane models, liposomes were added to a total concentration of 2 mM. Measurements were performed by using a quartz cell with the path length of 1 mm on an Olis DSM 1000 CD spectrophotometer (Olis), and data were collected at 1.0 nm intervals. All spectra were obtained at far-UV wavelengths (195–250 nm) as the average of five scans followed by background subtraction. Measurements were monitored to ensure that the HV values did not exceed 700. All spectra were smoothed by using an 11-point second-order Savitzky–Golay routine. The raw data,  $\theta_{\text{degrees}}$  were converted by using the equation  $\text{MRE} = \theta_{\text{degrees}} / (\text{path length in mm} \times \text{the molar concentration} \times \text{the number of residues})$ .<sup>42</sup>

## ■ ASSOCIATED CONTENT

### ● Supporting Information

HPLC chromatograms, NMR spectra, and data from the MTS/PMS assay. This material is available free of charge via the Internet at <http://pubs.acs.org>.

## ■ AUTHOR INFORMATION

### Corresponding Author

\*Phone: +45 3533 6255. Fax: +45-35336041. E-mail: hf@farma.ku.dk.

### Notes

The authors declare no competing financial interest.

## ■ ACKNOWLEDGMENTS

We thank Kenneth Johansen and Sileshi G. Wubshet for assistance during the LC-HRMS experiments as well as Birgitte Simonsen for excellent technical assistance. We also thank Anne Sandberg-Schaal for carrying out the investigations of hemolytic activity and Jytte Mark Andersen for assistance during investigations of the MICs. Finally, we thank Hanne Mørck Nielsen for providing resources for the cytotoxicity investigations as well as the liposome preparation. The present work is performed as a part of the Danish Center for Antibiotic Research and Development (DanCARD) financed by The Danish Council for Strategic Research (grant no. 09-067075).

## ■ ABBREVIATIONS USED

aa, amino acid; AMP, antimicrobial peptide; Boc, *tert*-butoxycarbonyl; DCM, dichloromethane; DIC, *N,N'*-diisopropylcarbodiimide; DIPEA, diisopropylethylamine; EMEM, Eagle's Minimal Essential Medium; ESBL, extended-spectrum β-lactamase; Fmoc, fluorenylmethoxycarbonyl; HA, hemolytic activity; HBSS, Hank's Balanced Salt Solution; hBRC, human red blood cells; HBTU, 2-(1*H*-benzotriazol-1-yl)-1,1,3,3-tetramethyluronium hexafluorophosphate; HOAt, 7-aza-1-hydroxybenzotriazole; HOBt, 1-hydroxybenzotriazole; KPC, *K. pneumoniae* carbapenemase; LUV, large unilamellar phospholipid vesicles; MDR, multidrug-resistant; MRE, mean residue ellipticity; MRSA, methicillin-resistant *Staphylococcus aureus*; MTS/PMS, 3-(4,5-dimethylthiazol-2-yl)-5-(3-carboxymethoxyphenyl)-2-(4-sulfophenyl)-2*H*-tetrazolium/phenazine methosulphate; MW, microwave; NCCLS/CLSI, National Committee for Clinical Laboratory Standards/Clinical and Laboratory Standards Institute; NDM-1, New Delhi metallo-β-lactamase-1; POPC, 1-palmitoyl-2-oleoyl-*sn*-glycero-3-phosphocholine; POPG, 1-palmitoyl-2-oleoyl-*sn*-glycero-3-phosphoglycerol; PyBOP, (benzotriazol-1-yl)oxytripyrrolidinophosphonium hexafluorophosphate; SDS, sodium dodecyl sulfate; SPPS, solid-phase peptide synthesis; Su, succinimidyl; TBS, tris-buffered saline; TFFH, tetramethylfluoroformamidinium hexafluorophosphate; TI, therapeutic index; VLC, vacuum liquid chromatography

## ■ REFERENCES

- (1) ECDC. *Annual Report of the European Antimicrobial Resistance Surveillance Network*; European Centre for Disease Prevention and Control: Stockholm, 2010.
- (2) WHO. *Impacts of Antimicrobial Growth Promoter Termination in Denmark*; WHO/CDS/CPE/ZFK/2003.1; World Health Organization: Foulum, 2003.
- (3) Projan, S. J. Why is Big Pharma getting out of antibacterial drug discovery? *Curr. Opin. Microbiol.* **2003**, *6*, 427–430.
- (4) Hammerum, A. M.; Lester, C. H.; Jakobsen, L.; Porsbo, L. J. Faecal carriage of extended-spectrum β-lactamase-producing and AmpC β-lactamase-producing bacteria among Danish army recruits. *Clin. Microbiol. Infect.* **2011**, *17*, 566–568.
- (5) Campos, J.; Oteo, J.; Perez-Vazquez, M. Extended-spectrum β-lactamase producing *Escherichia coli*: changing epidemiology and clinical impact. *Curr. Opin. Infect. Dis.* **2010**, *23*, 320–326.



- (6) Nordmann, P.; Poirel, L.; Lagrutta, E.; Taylor, P.; Pham, J. Emergence of Metallo- $\beta$ -Lactamase NDM-1-Producing Multidrug-Resistant *Escherichia coli* in Australia. *Antimicrob. Agents Chemother.* **2010**, *54*, 4914–4916.
- (7) Talbot, G. H.; Bradley, J.; Edwards, J. E.; Gilbert, D.; Scheld, M.; Bartlett, J. G. Bad Bugs Need Drugs: An Update on the Development Pipeline from the Antimicrobial Availability Task Force of the Infectious Diseases Society of America. *Clin. Infect. Dis.* **2006**, *42*, 657–668.
- (8) Paterson, D. L. Resistance in Gram-negative bacteria: *Enterobacteriaceae*. *Am. J. Infect. Control* **2006**, *34*, S20–S28 discussion S64–S73.
- (9) Zasloff, M. Antimicrobial peptides of multicellular organisms. *Nature* **2002**, *415*, 389–395.
- (10) Hancock, R. E.; Sahl, H. G. Antimicrobial and host–defense peptides as new anti-infective therapeutic strategies. *Nature Biotechnol.* **2006**, *24*, 1551–1557.
- (11) Rotem, S.; Mor, A. Antimicrobial peptide mimics for improved therapeutic properties. *Biochim. Biophys. Acta, Biomembr.* **2009**, *1788*, 1582–1592.
- (12) Hamuro, Y.; Schneider, J. P.; DeGrado, W. F. De Novo Design of Antibacterial  $\beta$ -Peptides. *J. Am. Chem. Soc.* **1999**, *121*, 12200–12201.
- (13) Zuckermann, R. N.; Kerr, J. M.; Kent, S. B. H.; Moos, W. H. Efficient method for the preparation of peptoids [oligo(*N*-substituted glycines)] by submonomer solid-phase synthesis. *J. Am. Chem. Soc.* **1992**, *114*, 10646–10647.
- (14) Hamper, B. C.; Kolodziej, S. A.; Scates, A. M.; Smith, R. G.; Cortez, E. Solid Phase Synthesis of  $\beta$ -Peptoids: *N*-Substituted  $\beta$ -Aminopropionic Acid Oligomers. *J. Org. Chem.* **1998**, *63*, 708–718.
- (15) Schmitt, M. A.; Weisblum, B.; Gellman, S. H. Interplay among folding, sequence, and lipophilicity in the antibacterial and hemolytic activities of  $\alpha/\beta$ -peptides. *J. Am. Chem. Soc.* **2007**, *129*, 417–428.
- (16) Ryge, T. S.; Fridomdt-Møller, N.; Hansen, P. R. Antimicrobial activities of twenty lysine-peptoid hybrids against clinically relevant bacteria and fungi. *Chemotherapy* **2008**, *54*, 152–6.
- (17) Chongsirawatana, N. P.; Patch, J. A.; Czyzewski, A. M.; Dohm, M. T.; Ivankin, A.; Gidalevitz, D.; Zuckermann, R. N.; Barron, A. E. Peptoids that mimic the structure, function, and mechanism of helical antimicrobial peptides. *Proc. Natl. Acad. Sci. U.S.A.* **2008**, *105*, 2794–2799.
- (18) Olsen, C. A.; Ziegler, H. L.; Nielsen, H. M.; Fridomdt-Møller, N.; Jaroszewski, J. W.; Franzyk, H. Antimicrobial, hemolytic, and cytotoxic activities of  $\beta$ -peptoid-peptide hybrid oligomers: improved properties compared to natural AMPs. *ChemBioChem* **2010**, *11*, 1356–60.
- (19) Olsen, C. A.; Bonke, G.; Vedel, L.; Adersen, A.; Witt, M.; Franzyk, H.; Jaroszewski, J. W.  $\alpha$ -Peptide/ $\beta$ -peptoid chimeras. *Org. Lett.* **2007**, *9*, 1549–1552.
- (20) Park, K. H.; Nan, Y. H.; Park, Y.; Kim, J. I.; Park, I. S.; Hahm, K. S.; Shin, S. Y. Cell specificity, anti-inflammatory activity, and plausible bactericidal mechanism of designed Trp-rich model antimicrobial peptides. *Biochim. Biophys. Acta, Biomembr.* **2009**, *1788*, 1193–1203.
- (21) Bonke, G.; Vedel, L.; Witt, M.; Jaroszewski, J. W.; Olsen, C. A.; Franzyk, H. Dimeric building blocks for solid-phase synthesis of  $\alpha$ -peptide- $\beta$ -peptoid chimeras. *Synthesis* **2008**, 2381–2390.
- (22) Kruijtzer, J. A. W.; Hofmeyer, L. J. F.; Heerma, W.; Versluis, C.; Liskamp, R. M. J. Solid-phase syntheses of peptoids using Fmoc-protected *N*-substituted glycines: The synthesis of (retro) peptoids of Leu-enkephalin and substance P. *Chem.—Eur. J.* **1998**, *4*, 1570–1580.
- (23) Noack, M.; Göttlich, R. Iodide-Catalysed Cyclization of Unsaturated *N*-Chloroamines: A New Way to Synthesize 3-Chloroperidines. *Eur. J. Org. Chem.* **2002**, 3171–3178.
- (24) Østergaard, S.; Holm, A. Peptomers: A Versatile Approach for the Preparation of Diverse Combinatorial Peptidomimetic Bead Libraries. *Mol. Divers.* **1997**, *3*, 17–27.
- (25) Zhang, X. A.; Oglecka, K.; Sandgren, S.; Belting, M.; Esbjerner, E. K.; Norden, B.; Graslund, A. Dual functions of the human antimicrobial peptide LL-37-Target membrane perturbation and host cell cargo delivery. *Biochim. Biophys. Acta, Biomembr.* **2010**, *1798*, 2201–2208.
- (26) Godballe, T.; Nilsson, L. L.; Petersen, P. D.; Jenssen, H. Antimicrobial  $\beta$ -Peptides and  $\alpha$ -Peptoids. *Chem. Biol. Drug. Des.* **2011**, *77*, 107–116.
- (27) ECDC. *Annual Epidemiological Report 2011*; European Centre for Disease Control and Prevention: Stockholm, 2011.
- (28) ECDC. *Updated Risk Assessment on the Spread of NDM and Its Variants within Europe*; European Centre for Disease Prevention and Control: Stockholm, 2011.
- (29) Jenssen, H.; Hamill, P.; Hancock, R. E. W. Peptide Antimicrobial Agents. *Clin. Microbiol. Rev.* **2006**, *19*, 491–511.
- (30) Wu, C. W.; Sanborn, T. J.; Huang, K.; Zuckermann, R. N.; Barron, A. E. Peptoid Oligomers with  $\alpha$ -Chiral, Aromatic Side Chains: Sequence Requirements for the Formation of Stable Peptoid Helices. *J. Am. Chem. Soc.* **2001**, *123*, 6778–6784.
- (31) Wu, C. W.; Kirshenbaum, K.; Sanborn, T. J.; Patch, J. A.; Huang, K.; Dill, K. A.; Zuckermann, R. N.; Barron, A. E. Structural and Spectroscopic Studies of Peptoid Oligomers with  $\alpha$ -Chiral Aliphatic Side Chains. *J. Am. Chem. Soc.* **2003**, *125*, 13525–13530.
- (32) Mowery, B. P.; Lee, S. E.; Kissounko, D. A.; Epand, R. F.; Epand, R. M.; Weisblum, B.; Stahl, S. S.; Gellman, S. H. Mimicry of antimicrobial host–defense peptides by random copolymers. *J. Am. Chem. Soc.* **2007**, *129*, 15474–15476.
- (33) Martinek, T. A.; Fülöp, F. Side-chain control of  $\beta$ -peptide secondary structures. *Eur. J. Biochem.* **2003**, *270*, 3657–3666.
- (34) Simon, R. J.; Kania, R. S.; Zuckermann, R. N.; Huebner, V. D.; Jewell, D. A.; Banville, S.; Ng, S.; Wang, L.; Rosenberg, S.; Marlowe, C. K. Peptoids: a modular approach to drug discovery. *Proc. Natl. Acad. Sci. U.S.A.* **1992**, *89*, 9367–9371.
- (35) Hansen, T.; Alst, T.; Havelkova, M.; Strøm, M. B. Antimicrobial Activity of Small  $\beta$ -Peptidomimetics Based on the Pharmacophore Model of Short Cationic Antimicrobial Peptides. *J. Med. Chem.* **2009**, *53*, 595–606.
- (36) Chen, Y. X.; Mant, C. T.; Farmer, S. W.; Hancock, R. E. W.; Vasil, M. L.; Hodges, R. S. Rational design of  $\alpha$ -helical antimicrobial peptides with enhanced activities and specificity/therapeutic index. *J. Biol. Chem.* **2005**, *280*, 12316–12329.
- (37) Zhu, W. L.; Song, Y. M.; Park, Y.; Park, K. H.; Yang, S. T.; Kim, J. I.; Park, I. S.; Hahm, K. S.; Shin, S. Y. Substitution of the leucine zipper sequence in melittin with peptoid residues affects self-association, cell selectivity, and mode of action. *Biochim. Biophys. Acta, Biomembr.* **2007**, *1768*, 1506–1517.
- (38) Slaninová, J.; Mlsová, V.; Kroupová, H.; Alán, L.; Tůmová, T.; Monincová, L.; Borovičková, L.; Fučík, V.; Čerovský, V. Toxicity study of antimicrobial peptides from wild bee venom and their analogs toward mammalian normal and cancer cells. *Peptides* **2012**, *33*, 18–26.
- (39) Mygind, P. H.; Fischer, R. L.; Schnorr, K. M.; Hansen, M. T.; Sonksen, C. P.; Ludvigsen, S.; Raventos, D.; Buskov, S.; Christensen, B.; De Maria, L.; Taboureau, O.; Yaver, D.; Elvig-Jorgensen, S. G.; Sorensen, M. V.; Christensen, B. E.; Kjaerulf, S.; Fridomdt-Møller, N.; Lehrer, R. I.; Zasloff, M.; Kristensen, H.-H. Plectasin is a peptide antibiotic with therapeutic potential from a saprophytic fungus. *Nature* **2005**, *437*, 975–980.
- (40) Hope, M. J.; Bally, M. B.; Webb, G.; Cullis, P. R. Production of Large Unilamellar Vesicles by a Rapid Extrusion Procedure—Characterization of Size Distribution, Trapped Volume and Ability to Maintain a Membrane-Potential. *Biochim. Biophys. Acta* **1985**, *812*, 55–65.
- (41) Foged, C.; Franzyk, H.; Bahrami, S.; Frokjaer, S.; Jaroszewski, J. W.; Nielsen, H. M.; Olsen, C. A. Cellular uptake and membrane-destabilising properties of  $\alpha$ -peptide/ $\beta$ -peptoid chimeras: lessons for the design of new cell-penetrating peptides. *Biochim. Biophys. Acta, Biomembr.* **2008**, *1778*, 2487–2495.
- (42) Greenfield, N. J. Using circular dichroism spectra to estimate protein secondary structure. *Nature Protoc.* **2006**, *1*, 2876–2890.